A graph-based framework for steady-state load flow analysis of multi-carrier

Markensteijn, A.S.; Romate, Johan; Vuik, C.

Publication date
2019

Document Version
Final published version

Citation (APA)
Markensteijn, A. S., Romate, J., & Vuik, C. (2019). *A graph-based framework for steady-state load flow analysis of multi-carrier*. (Reports of the Delft Institute of Applied Mathematics; Vol. 19-01). Delft University of Technology.

DELFT UNIVERSITY OF TECHNOLOGY

REPORT 19-01

A graph-based framework for steady-state load flow analysis of multi-carrier energy networks

A.S. Markensteijn, J.E. Romate, C. Vuik

ISSN 1389-6520

Reports of the Delft Institute of Applied Mathematics

Delft 2019

A graph-based framework for steady-state load flow analysis of multi-carrier energy networks

A.S. Markensteijn, J.E. Romate, C. Vuik

March 14, 2019

Abstract

Energy systems are becoming more complex due to increased coupling between different networks, resulting in multi-carrier energy networks. Conventional models for the separate networks are not able to capture the full extend of the coupling. Recently, different models for multi-carrier networks have been proposed, either using the energy hub concept or using a case specific approach. Although the energy hub concept can be applied to a general integrated network, it is unclear how the energy hub should be represented in the graph of the multi-carrier network. This paper presents a graph-based framework for steady-state load flow models of multi-carrier energy systems. Furthermore, the effect of coupling on the integrated system of equations is investigated. The proposed framework is tested on two small multi-carrier networks, for comparison with models in literature. Results show that our framework is applicable to a general system, and that it generalizes both the energy hub concept and the case specific approaches.

1 Introduction

Multi-carrier energy systems (MES) have become more important over the years as the need for efficient, reliable and low carbon energy systems increases. In MES, different energy carriers, such as electricity and heat, interact with each other leading to one combined system. They have higher performance than classical single-carrier energy systems due to increased flexibility, reliability, use of renewables and distributed generation, and reduced carbon emission. Because these multi-carrier energy systems integrate two or more separate energy systems they are sometimes called integrated energy systems. An overview of MES is given by Mancarella [2014].

An important tool for designing and operating energy systems is steady-state energy flow analysis (also called power flow or load flow analysis) of the energy transportation and distribution networks. This analysis determines the network state parameters and the flow of energy in the network. Load flow models for single-carrier network have been well studied. Recently, different models have been proposed to model load flow for MES. Two types of models can be distinguished. The first uses the energy hub concept, the other a more ad hoc approach.

The energy hub concept was first introduced by Geidl and Andersson [2007] to model the relation between different energy carriers, and to optimize MES. The input and output energy of the hub are related through a coupling matrix. Unidirectional flow from input to output is assumed,

such that the coupling matrix is constant or a function of the input power only. Within the energy hub, the transmission of energy carriers is not taken into account. Wasilewski [2015] and Long et al. [2017] extend the energy hub concept to allow bidirectional flow, based on graph and network theory. They provide different detailed graph representations of energy flow within an energy hub. However, connecting the energy hub to the rest of the energy network is not described, such that the network state parameters in the single-carrier parts of the network are not modeled. Ayele et al. [2018] extend the energy hub concept by explicitly modeling the connection between the energy hub and the rest of the energy network. All local energy generation is included in the hub. Their model determines network state parameters in the single-carrier parts. However, the output power of the hub is assumed to be a linear function of the input power. Moreover, the energy hub is not seen as a node or an edge, such that the graph representation of the energy hub is unclear.

The second type of model combines the existing model equations of the single-carrier networks into one system of equations. This way of modeling provides both the energy flow through a network and the network state parameters, and allows the use of detailed models for the conversion and transmission of energy. An et al. [2003] introduced such a model for a combined gas and electricity network, and Liu et al. [2016] introduced one for a combined heat and electricity network. Martinez-Mares and Fuerte-Esquivel [2012] introduced a model for a combined electricity and gas network, using a distributed slack node approach in the electricity network, and taking into account temperature effects in the gas network. Pan et al. [2016] introduced a model for a combined electricity and heat network, taking the different time scales in the heat network into account. More recently, Shabanpour-Haghighi and Seifi [2015] and Abeysekera and Wu [2015] both gave models for a combined gas, electricity, and heat network. Furthermore, Liu and Mancarella [2016] extended the previous work of Liu et al. [2016] to also include gas. However, these models are case specific and are therefore difficult to apply to a general integrated energy network.

Jalving et al. [2017] proposed a general graph-based computational framework for optimizing combined networks, which they apply to a combined electricity and gas network. The load flow equations are part of the constraints, such that steady-state load flow analysis is considered a special case of their proposed optimization model. They assume that a feasible solution, satisfying these constraints, exists. However, some coupling models and single-carrier load flow equations can lead to a combined system which has no (feasible) solution.

To the best of the authors' knowledge the current load flow models provide a case specific approach for a load flow problem of MES, or a general model for the conversion of one carrier into another. Most do not state how the graphs of single-carrier networks can be combined into one multi-carrier network. Moreover, they do not consider the effect of this combination on the load flow model for a MES. Usually, the coupling models introduce more unknowns than equations to the system. Therefore, additional equations or boundary conditions must be added for the system to be (uniquely) solvable. Depending on how the single-carrier networks are connected to form an integrated network, and depending on the choice of the additional equations, the resulting system of load flow equations might have none, one, or infinite solutions. A systematic analysis of the single-carrier load flow models and graphs, and of possible graph representations of the multi-carrier system, is important to identify and understand these ill-posed systems. Therefore, we propose a general load flow model framework for multi-carrier energy networks, based on graph and network theory.

We propose a graph representation for MES, and provide guidelines for combining the single-carrier load flow models with conversion models, into one multi-carrier load flow model. The graph representation of single-carrier and multi-carrier networks is presented in Section 2. The integrated load flow model is discussed in Section 3. A case study consisting of a gas network, power grid (electrical network), and a heating network is provided in Section 4. This case study is based on the ones by Shabanpour-Haghighi and Seifi [2015] and Ayele et al. [2018] for comparison. Furthermore, it provides insight into the difficulties of combining single-carrier load flow models and conversion models. Some concluding remarks are given in Section 5.

2 Graph-representation

Energy networks all have their own terminology. For instance, an electrical network is usually called a power grid. This specific terminology also extends to the elements of a network. For instance, a basic power grid consists of power lines connected by buses, whereas a gas pipeline network consists of pipelines connected by junctions. Mathematically, all networks are abstracted to a graph. Some terms and definitions of graphs and energy networks are given below.

2.1 Terms and definitions

An *(undirected) graph* $\mathcal{G}$ is a pair $(\mathcal{V}, \mathcal{E})$ where $\mathcal{V}$ is a set of *nodes* or *vertices* v_i and $\mathcal{E}$ is a set of *links* or *edges* e_k. An edge is itself a set of two nodes such that $e_k = \{v_i, v_j\}$. We denote the size of a set $\mathcal{S}$ by $|\mathcal{S}|$. A *directed graph* $\mathcal{G}$ is a pair $(\mathcal{V}, \mathcal{E})$ where $\mathcal{V}$ is again a set of nodes. $\mathcal{E}$ is a set of *arcs* e_k, where an arc is an ordered pair of nodes $e_k = (v_i, v_j)$. Thus, an arc is a link with a predefined direction. The actual direction of flow through the link could be opposite to this direction. Arcs are also referred to as edges or links.

Inflow and outflow of a network are usually represented by special nodes called *sources* and *sinks* respectively. However, this representation is difficult to use for energy networks. First, it is sometimes impossible to know up front if a node represents an inflow or outflow of energy. Secondly, in modeling it is convenient to see the inflow and outflow of a node as a flow through a link. Therefore, we introduce *terminal nodes* and *terminal links*.

A terminal node is a node that can act as both a source or a sink, depending on the direction of the terminal link. A terminal link is a special type of link that has no physical model, and is only connected to one node. It is sometimes called a *half-edge* and can be denoted by $t_l = \{v_i\}$. A terminal link is simply a representation of flow entering or leaving the network. Hence, by definition, a terminal link can only be connected to a terminal node. Moreover, connecting a terminal link to any node turns that node into a terminal node. Conversely, a node without a terminal link connected to it is not a terminal node. One node can have more than one terminal link connected to it. We denote the set of terminal links in the graph by $\mathcal{T}$, and the set of terminal links connected to a node $v \in \mathcal{V}$ by $\mathcal{T}(v)$.

A network can then be represented as a collection of nodes, (directed) links, and terminal links, such that $\mathcal{N} = \{\mathcal{V}, \mathcal{E}, \mathcal{T}\} = \{\mathcal{G}, \mathcal{T}\}$. If $\mathcal{G}$ is a directed graph the network is said to be directed, and it is said to be undirected if $\mathcal{G}$ is an undirected graph.

One property of graphs that is used for modeling energy networks is the incidence matrix. For an undirected graph $\mathcal{G} = (\mathcal{V}, \mathcal{E})$ the elements of the $|\mathcal{V}| \times |\mathcal{E}|$ incidence matrix A are defined as

$$A_{ik} = \begin{cases} 1, \text{ if } e_k = \{v_i, v_j\} \\ 0, \text{ otherwise} \end{cases} \tag{1}$$

for every link $e_k \in \mathcal{E}$ and every node $v_i \in \mathcal{V}$. Similarly, for a directed graph the elements of the incidence matrix are defined as

$$A_{ik} = \begin{cases} 1, \text{ if } e_k = (v_j, v_i) \\ -1, \text{ if } e_k = (v_i, v_j) \\ 0, \text{ otherwise} \end{cases} \tag{2}$$

for every link $e_k \in \mathcal{E}$ and every node $v_i \in \mathcal{V}$.

2.2 Single-carrier energy systems

Usually, a gas network and a heat network are represented by a directed graph, whereas a balanced AC power grid is represented by an undirected graph. The representation of the heat network as a directed graph is less straightforward and is explained below in more detail.

The physical pipeline system of a heat network consists of a supply part (supplying warm water to demands) and a return part (returning cold water to sources). These two parts are connected to each other through the (heat) loads and sources. Heat is then injected or consumed through heat exchangers Frederiksen and Werner [2014]. Figure 1a gives a model representation of a source and a load connected with pipes. This means that the hydraulic part of the heat network is a closed system. For most classical heat networks it can be assumed that the water flow through the return lines is opposite in direction, but equal in size, to the water flow in the supply line [Kuosa et al., 2013]. This means that the return line does not have to be modeled explicitly, so that a source connected with a pipe to a load can be abstracted to a directed graph, with terminal links, as shown in Figure 1b. Note that in this representation the (hydraulic part) of the heat network is no longer a closed system.

For every network, variables are associated with the links and nodes in the graph. For basic steady-state load flow, these are pressure p and flow q for a gas network, voltage V, current I, and complex power S for a power grid, and head h, water flow m, heat power φ, supply temperature T^s, return temperature T^r, and outflow temperature T^o for a heat network. Table 1 gives an overview of these variables and the graph element they are associated with. The variables associated with a terminal link can be seen as variables of the terminal node. To distinguish between (terminal) link and terminal node variables, the ones on the terminal node are called *injected*. If a node has more than one terminal link connected to it, then the injected flow or power is the sum of the flows and powers of the terminal links.

For the basic load flow equations (see Section 3) it is convenient to associate some of the link and node variables with the beginning or end of a link, directly next to a node. Figures 1b, 2a, and 2b show the graph representation for each of the three single-carrier networks. They show a source

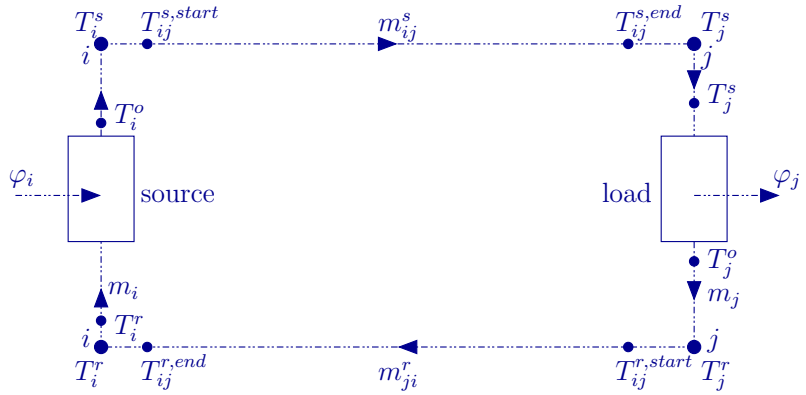

(a) Model representation.

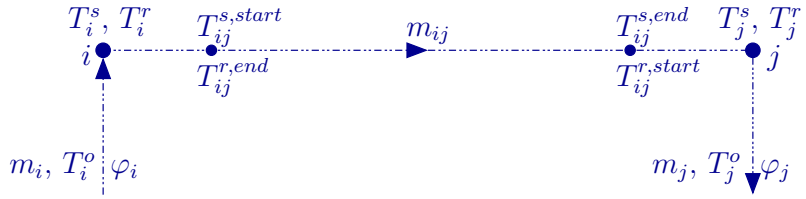

(b) Graph representation.

Figure 1: A heat network with a source, represented by node i, connected to a load, represented by node j, using one heat pipe. (a) shows a more realistic model representation with both the supply and return line. (b) shows the graph representation with only the supply line, represented by an arc, and the load and source, represented by terminal links. T is the temperature, m the mass flow, and φ the heat power.

Table 1: Variables for a gas, heat, and electrical network, per graph element they are associated with.

Network	Node	Link	Terminal node
Gas	pressure p	flow q	injected flow q
Heat	head h	flow m	injected flow m
	supply temperature T^s		outflow temperature T^o
	return temperature T^r		heat power φ
Electricity	voltage V	current I	injected current I
			injected complex power S

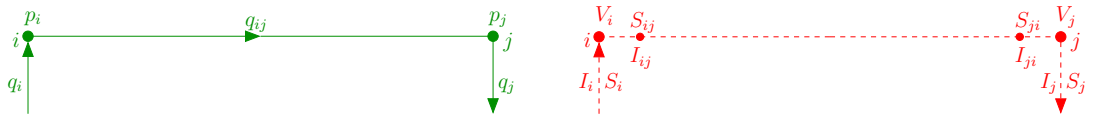

(a) Gas network.

(b) Power grid.

Figure 2: Graph representation of a source, represented by node i, connected to a load, represented by node j, by one link. The variables used in load flow analysis are shown at the location in the graph where they are modeled. (a) shows a gas network with p pressure and q volume flow. (b) shows a power grid with I current, V voltage, and S complex power.

connected with one link to a sink, and the variables at the location in the graph where they are modeled. A line in a power grid (see Figure 2b) does not have one single link current, but one at each side of a link. For most transmission line models it holds that $I_{ij} \neq -I_{ji}$, whereas $q_{ij} = -q_{ji}$ and $m_{ij} = -m_{ji}$ for pipelines.

2.3 Coupling of energy systems

Wasilewski [2015] proposes a detailed graph representation of an energy hub, allowing for bidirectional flow. It uses directed edges and terminal nodes to form energy converter graphs and energy storage graphs. Long et al. [2017] also extend the energy hub concept to allow bidirectional flow by introducing a *MES node*, consisting of an energy conversion model, a storage model, and a prosumer model. The conversion model is represented by a graph consisting of *terminal nodes*, *sum nodes*, and *transmitter nodes*. Nodes are associated with an energy carrier, such that conversion of one energy carrier to another is represented by a directed edge. However, both only consider energy flow and do not describe how the energy hub should be connected to the rest of the network. Ayele et al. [2018] connect the energy hub with the rest of the network using a node called the *point of interconnection*. The energy hub, consisting of demand, local generation, edges, and a *coupling system*, is not seen as a node or an edge. However, a graph is a collection of nodes and links, which holds for the abstraction of any energy system, both single-carrier and multi-carrier. Coupling single-carrier networks to form a multi-carrier network can therefore only be done through (a combination of) nodes or links.

There are three main options to couple two nodes: connect the two nodes by a link, merge the two nodes into one node, or introduce an additional node and connect the two nodes to it. Since a link is a component that has two flow connections, it is difficult to use a link to model a coupling that involves more than two energy carriers such as a combined heat and power plant. Furthermore, the physical interpretation of a coupling link is not straightforward. Coupling two nodes by merging them into one is difficult because of the parameters associated with the nodes. For instance, suppose we want to connect two gas networks by merging one node of each network with each other into one new gas node. Both nodes have a pressure associated with them, which means some combined pressure must be defined for the new gas node, or gas nodes with multiple pressures must be allowed. When we want to couple two networks of different energy carriers this problem becomes even more clear. Additionally, merging two nodes of a different energy carrier would require some adaptation of Kirchhoff's law, for instance to distinguish between the links connected to the node (see Section 3 for more details on Kirchhoff's law). Therefore, we choose to couple networks by

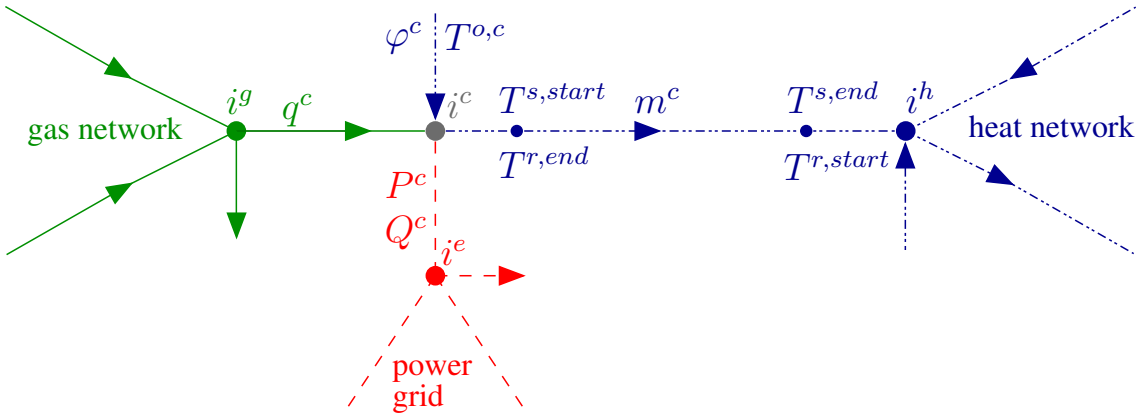

Figure 3: Coupling node i^c (gray), connected by dummy links to node i^g of a gas network (solid green), node i^e of a power grid (dashed red), and node i^h of a heat network (dotted-dashed blue). The coupling parameters are shown next to the (terminal) links they are associated with. Here, q is gas volume flow, P is active power, Q is reactive power, T is temperature, m is water mass flow, and φ heat power.

introducing an additional node, called a *coupling node*.

For our model framework, no parameters are associated with a coupling node. Therefore, the coupling node does not belong to any of the single-carrier networks. We distinguish a *homogeneous coupling* node, which couples networks of the same energy carrier, and a *heterogeneous coupling* node, which couples networks with different energy carrier. Nodes and links of a single-carrier network are also said to be *homogeneous*. A network with one or more heterogeneous nodes is called heterogeneous, and conversely, a network without any heterogeneous node is called homogeneous. We focus on coupling networks of different energy carriers. A heterogeneous coupling node can have (terminal) links of different energy carriers connected to it. In theory, this could be any link, but since we do not define parameters on the coupling node, some links can not be connected to it. For instance, a gas link representing a pipeline has a (steady-state) flow equation associated with it, which gives a relation between the gas flow through the pipe and the pressures of the start and end node of the link (see Section 3 for more details). Since the coupling node has no pressure associated with it, such a gas link cannot be connected to it. We choose to connect the coupling node to homogeneous (single-carrier) nodes by *dummy links*. These links do not represent any physical component, they merely show a connection between nodes. However, they are homogeneous links and as such have the same parameters associated with them as any homogeneous link. The graph representation of a coupling node, connected to a single node of a gas network, a power grid, and a heat network is shown in Figure 3. The direction shown on the gas and heat dummy links and on the heat terminal links are the predefined directions of the links, which could be different from the actual direction of flow. Hence, the coupling node allows for bidirectional flow.

The coupling node can be used to represent something as relatively simple as a junction node

in gas network, or something as complex as a complete (heterogeneous) network. Representing another network, for instance the energy hub graph introduced by Wasilewski [2015], will lead to an hierarchical network. Such an hierarchical approach is used by Jalving et al. [2017], in their proposed computation framework. Furthermore, the proposed coupling node only needs to have inflow and outflow that can be represented by dummy links to connect it to the rest of the network. Due to the choice for dummy links, the integrated network could be separated easily into single-carrier parts by cutting the dummy links into two terminal links. This could be used to solve the integrated network in a decoupled way. This framework for coupling single-carrier networks allows great flexibility when connecting multiple networks, making it applicable to general multi-carrier energy networks.

3 Load flow models

The steady-state energy flow problem (also called power flow or load flow problem) is formulated by collecting the model equations of different physical components, which are in turn related to elements in the graph. There are two equations that hold for any (single-carrier) energy network: Kirchhoff's first and second laws. For every node, Kirchhoff's first law states that the total in- and outflow must sum up to zero. In a power grid this law is usually called Kirchhoff's current law, whereas in a gas and heat network it is conservation of mass or conservation of flow. For every loop in a network, Kirchhoff's second law states that the sum of potential differences over every link must be zero. In a power grid this law is usually called Kirchhoff's voltage law, whereas in a gas and heat network it is called the loop pressure equation. Additionally, most links are modeled by an equation that gives a relation between the link variable and the nodal variables. Different models are used, depending on what physical component is associated to the link. For instance, Ohm's law is used for a transmission line in a power grid. Some networks have additional node or link equations, such as the complex power equation in a power grid, which gives a relation between total injected current, total injected complex power, and nodal voltage.

3.1 Gas network

Assuming a steady-state approximation, a basic gas network can be completely described by a combination of the conservation of mass and a link equations that gives the relation between nodal pressures and link flow [Osiadacz, 1987]. For a general gas network, the conservation of flow is given by a linear system of equations:

$$A^g q - q^{\text{inj}} = 0 \tag{3}$$

with A^g the $|\mathcal{V}^g| \times |\mathcal{E}^g|$ incidence matrix of the gas network (2), q the vector of length $|\mathcal{E}^g|$ of link flows, and q^{inj} the vector of length $|\mathcal{V}^g|$ of injected flows. A link equation is then used to give the relation between nodal pressures and link flow:

$$f_k^g\left(q_k, p_i, p_j\right) = 0 \tag{4}$$

for every link $e_k^g \in \mathcal{E}^g$. These link equations are generally non-linear in the pressures. Combining the conservation of mass (3) and the link equations (4), and denoting with p the vector of length

$|\mathcal{V}^g|$ of nodal pressures, gives the following non-linear system of equations:

$$F^g\left(x^g\right) = \begin{pmatrix} A^g q - q^{\text{inj}} \\ f^g\left(q,p\right) \end{pmatrix} = 0 \quad \text{with} \quad x^g = \begin{pmatrix} q^{\text{inj}} \\ q \\ p \end{pmatrix} \tag{5}$$

This system consists of $|\mathcal{V}^g| + |\mathcal{E}^g|$ equations and $2|\mathcal{V}^g| + |\mathcal{E}^g|$ unknowns. To reduce the number of unknowns, some nodal variables are assumed known. We will refer to this as the *boundary conditions* of the network. For basic load flow models, either the pressure or the total injected flow is given at every node. Furthermore, at least one of the equations of the conservation of mass (3) is a linear combination of the other equations. This means that if the injected flow is given at every node, the system of equations will generally not have a solution. If the pressure is not given for at least one node, there are infinite solutions, if a solution exists at all, because the link equations (4) are functions of the pressure drop. Hence, at one node the pressure is given while the injected flow is not known. This pressure is called the *reference pressure* and this node is called the *reference node*. A node where the injected flow is given while the pressure is not known is called a *load node*. Nodes where both the pressure and the injected flow are given, or nodes where neither are given, can also occur. We call them a *reference load node* and a *slack node* respectively. The system of equations can be reformulated in different ways, based on for instance algebraic substitutions. The most common ones are the nodal formulation, the loop formulation, and the nodal-loop formulation. See for instance Osiadacz [1987] for details, advantages, and disadvantages of each formulation.

3.2 Power grid

Assuming an AC steady-state approximation, a power grid is completely described by a combination of Kirchhoff's current law, a link equation that gives a relation between nodal voltage and link current (e.g. Ohm's law), and the complex power equation [Schavemaker and Van der Sluis, 2008]. For a general power grid, Kirchhoff's current law is given by a linear system of equations:

$$A^e I - I^{\text{inj}} = 0 \tag{6}$$

with A^e the incidence matrix of the power grid (1), I the vector of complex currents, and I^{inj} the vector of injected complex currents. A link equation is then used to give the relation between nodal voltages V_i and V_j, and link current I_k:

$$f_k^e\left(I_k, V_i, V_j\right) = 0 \tag{7}$$

for every link $e_k^e \in \mathcal{E}^e$. Finally, the complex power equation is given by a non-linear equation in I and V:

$$S^{\text{inj}} = V\left(I^{\text{inj}}\right)^* \tag{8}$$

where $[\cdot]^*$ denotes the complex conjugate. Combining Kirchhoff's current law (6), the link equations (7), and the complex power equations (8) gives the following non-linear system of equations:

$$F^e\left(x^e\right) = \begin{pmatrix} A^e I - I^{\text{inj}} \\ f^e\left(I,V\right) \\ S^{\text{inj}} - V\left(I^{\text{inj}}\right)^* \end{pmatrix} = 0 \quad \text{with} \quad x^e = \begin{pmatrix} I^{\text{inj}} \\ I \\ V \\ S^{\text{inj}} \end{pmatrix} \tag{9}$$

Because all parameters associated with an AC power grid are complex, this system consists of $4|\mathcal{V}^e| + 2|\mathcal{E}^e|$ equations and $6|\mathcal{V}^e| + 2|\mathcal{E}^e|$ variables. The complex power S is usually split in its real and imaginary part. The real part is called the active power P, and imaginary part the reactive power Q. The voltage V is split in its angle δ and amplitude $|V|$. Again, boundary conditions are introduced to reduce the number of unknowns. For classic load flow, two variables are given at each node: P^{inj} and Q^{inj} for a *load node*, P^{inj} and $|V|$ for a *generator node*, or $|V|$ and δ for a *reference node*. The reference node is introduced for similar reasons as for the gas network; for at least one node the injected complex power must be unknown, and for at least one node the voltage must be given. Mathematically, any other combination of known or unknown nodal variables could be used, for instance a $Q\delta$-node with known injected reactive power Q and nodal voltage angle δ. However, from a technical perspective, only the first three nodes are the feasible node types [Schavemaker and Van der Sluis, 2008].

The system of equations with boundary conditions can be reformulated in different ways, but the most common is the complex power formulation (using polar coordinates) (e.g. Schavemaker and Van der Sluis [2008], Idema et al. [2010]). For other possible formulations, see for instance [Stott, 1974] or [Sereeter et al., 2017].

3.3 Heat network

A heat network consist of a hydraulic part and a thermal part. Assuming a steady-state approximation, the hydraulic part is completely described by a combination of conservation of mass and a link equation. The thermal part is completely described by a nodal mixing-rule, a link equation to relate mass flow to temperatures, and a heat power equation [Bordin et al., 2016, Liu et al., 2016]. For a general heat network, the conservation of mass is given by a linear system of equations:

$$A^h m - m^{\text{inj}} = 0 \tag{10}$$

with A^h the incidence matrix of the heat network (2), m the vector of mass flows, and m^{inj} the vector of injected mass flows. As for gas, a link equation is used to give the relation between nodal heads h_i and h_j, and link mass flow m_k:

$$f_k^h\left(m_k, h_i, h_j\right) = 0 \tag{11}$$

for every link $e_k^h \in \mathcal{E}^h$. Again, these link equations are generally non-linear. The conservation of mass (10) combined with the link equations (11) gives the hydraulic model for the heat network.

The thermal model governs the temperatures in the supply lines, the return lines, and directly after a source or load, and the heat power injected by a source or consumed by a sink. We will assume that nodes are a *source*, a *sink*, or a *junction*. A source is a node with water inflow and heat power injection, and conversely a sink (or load) has water outflow and heat power consumption. A junction is a node in the network where the flow is redistributed, there is no connection between return and supply line, such that there is no water in- or outflow. For a component connected to a source or sink (that is, for a terminal link) the heat power equation holds:

$$f_{i,l}^{\varphi}\left(\varphi_{i,l}, m_{i,l}, T_i^s, T_i^r, T_{i,l}^o\right) = 0 \tag{12}$$

for every terminal link $t_l \in \mathcal{T}^h(v_i)$ connected to node $v_i \in \mathcal{V}^h$. Here, $\varphi_{i,l}$ is the injected or consumed heat power of terminal link t_l, $m_{i,l}$ is the injected mass flow, T_i^s is the supply temperature at node

v_i and T_i^r its return temperature, and $T_{i,l}^o$ is the temperature directly after the source or sink at terminal link t_l. The total injected mass flow of node v_i is then given by $m_i^{\text{inj}} = \sum_{t_l \in \mathcal{T}(v_i)} m_{l,i}$. At every node $v_i \in \mathcal{V}^h$, the temperature in the supply and return line are determined by the mixing rule, which states that the nodal temperature is the weighted average of the inflow temperatures:

$$\begin{aligned} f_i^{T^s} &= \left(\sum m_{\text{out}}^s\right) T_i^s - \left(\sum m_{\text{in}}^s T_{\text{in}}^s\right) = 0 \\ f_i^{T^r} &= \left(\sum m_{\text{out}}^r\right) T_i^r - \left(\sum m_{\text{in}}^r T_{\text{in}}^r\right) = 0 \end{aligned} \tag{13}$$

Here, $\sum m_{\text{out}}^s$ is used to denote the sum of all the outgoing flow of node i in the supply line, both on the edges and on the terminal links. Similarly, $\sum m_{\text{in}}^s$ denotes the sum of all ingoing flows of node i in the supply line, $\sum m_{\text{out}}^r$ the sum of all outgoing flows of node i in the return line, and $\sum m_{\text{in}}^r$ the sum of all ingoing flows of node i in the return line. It holds that $\sum m_{\text{in}}^r = \sum m_{\text{out}}^s$ and $\sum m_{\text{out}}^r = \sum m_{\text{in}}^s$. For every supply and every return pipeline, a link equation is used to give the relation between the temperatures at the beginning and end of the pipe and the pipe mass flow:

$$f_k^{\psi}\left(T_k^{\text{start}}, T_k^{\text{end}}, m_k\right) = 0 \tag{14}$$

The 'start' and 'end' of the pipeline are defined for the actual direction of flow, not with respect to the predefined direction of the directed link. Hence, $T_k^{s,\text{start}} = T_i^s$ if the flow through pipe k is from node i to node j, and $T_k^{s,\text{start}} = T_i^s$ if the direction of flow is in the opposite direction.

The heat power equation (12) combined with the mixing rule (13) and the link equation (14) gives the thermal model for the heat network. The hydraulic model and thermal model can be combined to one hydraulic-thermal model, given by the following, generally non-linear, system of equations:

$$F^h\left(x^h\right) = \begin{pmatrix} A^h m - m^{\text{inj}} \\ f^h\left(h, m\right) \\ f^{\varphi}\left(\varphi_l, m_l, T^s, T^r, T^o\right) \\ f^{T^s}\left(m, m_l, T^s, T^o\right) \\ f^{T^r}\left(m, m_l, T^r, T^o\right) \\ f^{\psi}\left(T^{s,\text{start}}, T^{s,\text{end}}, m\right) \\ f^{\psi}\left(T^{r,\text{start}}, T^{r,\text{end}}, -m\right) \end{pmatrix} = 0 \quad \text{with} \quad x^h = \begin{pmatrix} m_l \\ m \\ h \\ T^s \\ T^{s,end} \\ T^r \\ T^{r,end} \\ T^o \\ \varphi \end{pmatrix} \tag{15}$$

This system consists of $3|\mathcal{V}^h|+3|\mathcal{E}^h|+|\mathcal{T}^h|$ equations and $3|\mathcal{V}^h|+3|\mathcal{E}^h|+3|\mathcal{T}^h|$ variables. Boundary conditions are introduced to reduce the number of unknowns. Generally, at each source or sink node (at each terminal link) two variables are given: φ_l and T_l^o. These nodes are called a *source node* and a *load node* respectively. Because a circulation pump is usually located at a source, at one of the source nodes T^s and h are given. This head is then the reference head, and since the injected heat power is not known, this node is called a *source reference slack node*. We assume such a node has only one component (i.e. one terminal link) connected to it. Otherwise, for instance φ_l and T_l^o for all but one terminal link must be given. The source reference slack node is introduced

for much the same reasons as for the gas network and the power grid; for at least one node the injected heat power and mass flow must be unknown, and for at least one node the head must be given.

Again, the system of equations with boundary conditions can be reformulated in different ways. See for instance Liu et al. [2016] who consider the difference between the hydraulic-thermal model and separate hydraulic and thermal models, or Arsene et al. [1989] who compare the nodal and loop formulation of the hydraulic model.

3.4 Multi-carrier energy systems

3.4.1 Model

We couple homogeneous node(s) to a heterogeneous coupling node using dummy links. The dummy links do not represent any physical component, they only show a connection between nodes. However, they could be seen as lossless link, which means we could define the dummy links for the three single-carrier networks as follows. A gas dummy link does not have a link equation, it only has a gas flow q. A power dummy link has a complex current I for which it holds that $I_{ji} = -I_{ij}$. It also has active and reactive powers at the start and end of the line, for which it holds that $P_{ji} = -P_{ij} := P$ and $Q_{ji} = -Q_{ij} := Q$. Note that P and Q are independent of I and V (also because V is undefined for a heterogeneous node). A heat dummy link has a water flow m and supply and return temperature at the start and end of the link. Seeing it as a lossless line, it follows that $T_k^{\text{start}} = T_k^{\text{end}}$ for both supply and return. The coupling variables, denoted by $[\cdot]^c$, and their associated location in the graph are shown in Figure 3.

A heterogeneous coupling node has one or more node equations associated with it, that relate the different energy carriers to each other. We assume these *coupling equations* to be of the form

$$f^c\left(q^c, P^c, \varphi^c\right) = 0 \tag{16}$$

with q^c the vector of gas flows of all gas dummy links connected to the coupling node, P^c the vector of active powers of all power dummy links connected to the coupling node, and φ^c the vector of all heat powers of all heat terminal links connected to the coupling node. The heat terminal link represents some physical component that injects or consumes heat (with respect to the heat network), which means that there is a heat power equation (12) associated with it. Combining the coupling equations (16) with the heat power equation (12) gives the system of equation for all coupling nodes:

$$F^c\left(x^c\right) = \begin{pmatrix} f^c\left(q^c, P^c, \varphi^c\right) \\ f^\varphi\left(\varphi^c, m^c, T^s, T^r, T^{o,c}\right) \end{pmatrix} = 0 \quad \text{with} \quad x^c = \begin{pmatrix} q^c \\ P^c \\ Q^c \\ m^c \\ \varphi^c \\ T^{o,c} \end{pmatrix} \tag{17}$$

Since the dummy links used for coupling are homogeneous links, the system of equations for the single-carrier parts of the total integrated network are slightly altered (compared with before coupling). That is, the incidence matrices A^g, A^h, and A^g also include the dummy links. And, for heat,

the dummy links are also included in the mixing rules. However, the parameters of the dummy links are included in x^c, and not in x^g, x^e, or x^h.

Combining the systems of equations for the gas (5), power (9), heat (15), and coupling (17), gives a non-linear system of equations for the total integrated multi-carrier energy network:

$$F(x) = \begin{pmatrix} F^g\left(x^g, x^c\right) \\ F^e\left(x^e, x^c\right) \\ F^h\left(x^h, x^c\right) \\ F^c\left(x^c, x^h\right) \end{pmatrix} = 0 \quad \text{with} \quad x = \begin{pmatrix} x^g \\ x^h \\ x^e \\ x^c \end{pmatrix} \tag{18}$$

Due to the heterogeneous coupling node and the dummy links, this system of equations gets a specific structure. First, the equations belonging to the single-carrier parts do not directly depend on variables of the other single-carrier networks. All dependencies are incorporated through the coupling. Furthermore, F^g and F^e are linear in the coupling variables x^c (while F^h is non-linear in x^c because of the mixing rules (13)). Finally, the coupling system F^c depends on the heat parameters x^h, because the heat power equation of the terminal link depends on T^s (for a sink) or T^r (for a source) of the heat node connected to the coupling node (node i^h in Figure 3).

3.4.2 Node types

A coupling will usually introduce more variables than equations, such that (additional) boundary conditions must be introduced. One option is to impose these on the coupling part of the system, see for instance Shabanpour-Haghighi and Seifi [2015] who assume all heat powers to be known. However, assuming the coupling energy flows known will essentially decouple the system. For coupling components that produce heat, it is possible to assume $T^{o,c}$ known, as is done for any heat source or sink, without decoupling the systems. Another option is to impose the additional boundary conditions in the single-carrier parts of the network. This will introduce new node types. An overview of the new and standard node types is shown in Table 2.

To analyze the effect that coupling has on the node types, we assume that the systems of equations of the single-carrier networks are formulated such that (i.e., the boundary condition are chosen such that) they are solvable. Because a dummy link only represent an (energy) flow going into or out of a node, it could be seen as a terminal link from the perspective of the single-carrier networks. However, we will adopt the perspective of the total integrated multi-carrier network, in which the dummy links are just links. Node types are based on the boundary conditions, that is, based on which nodal variables are assumed known and which are assumed unknown. Therefore, having a dummy link connected to a homogeneous node does not change the node type. Adding additional boundary conditions in the single-carrier networks will.

A gas terminal node has only two nodal variables, pressure p and injected flow q. Assuming p, q, or both known at a node where it was originally unknown changes the node type. For instance, assuming the pressure known at a node that was originally a load node turns it into a reference load node. However, no new node types are found, since all possible node types are already used

in a single-carrier gas network.

For a power grid, the technically feasible node types are a load node, a generator node, or a reference node. However, at power nodes that are connected to a coupling node, the injected active or reactive power can be assumed known, since the unknown coupling power can serve as slack for that node. So a reference node can become a $PV\delta$, $QV\delta$, or $PQV\delta$ node, and a generator node can become a PQV node. Similar nodes were introduced by Martinez-Mares and Fuerte-Esquivel [2012], who consider a generator PV node with variable active power, and a generator PQ node with variable active power. Note that, unlike in the gas network, the additional boundary conditions cannot be imposed 'far' from the coupling in the power grid.

A heat terminal node has six nodal variables, meaning that many combinations of known and unknown variables exist, some of which are not technically feasible. We will only look at the effect of the coupling on the four most commonly used node types. The resulting node types will therefore not be the complete set of possibilities. Due to technical reasons it is uncommon to assume the injected mass flow to be known. Furthermore, it is unlikely that both T^s and T^r are known for one node. Furthermore, T^s for a source node, or T^r for a load node, can only be assumed known if $T^{o,c}$ is unknown. Then, $T^{o,c}$ will serve as 'slack' for the mixing rule. The original node types are then affected as follows. At a source node, assuming the head known leads to a *source reference node*, and assuming the supply temperature known leads to a *source temperature node*. Assuming the head known for a load node leads to a *load reference node* and for a junction to a *reference node*.

Usually T^o and φ are assumed known for every heat component (i.e. every terminal link), except for the source reference slack node. Assuming $T^{o,c}$ known for the terminal heat link connected to the coupling node does not decouple the system of equations, whereas assuming φ^c known would. Therefore, we will consider this a possible boundary condition on a coupling node.

Not all combinations of node types (that is, not all combinations of boundary conditions) lead to a solvable system. Even for a small single-carrier network, some combinations of node types will lead to a system with no solutions or a system with multiple solution. Consider a gas network consisting of a source connected with a pipe to a sink, such as shown in Figure 2a. If both node i and node j are load nodes, the system will have no solution if the boundary conditions are imposed such that $q_i \neq q_j$, and infinite solutions if $q_i = q_j$, because only the pressure drop can be determined. Assuming the node types in single-carrier networks were such that the load flow problem was (uniquely) solvable, imposing the additional boundary conditions after coupling could lead to an unsolvable system. For instance, one single-carrier network could become overdetermined while another becomes underdetermined. However, a necessary condition for a solvable system, with respect to the number of each node type, can be derived by requiring that the number of equations equals the number of variables.

3.4.3 Newton-Raphson method

Newton-Raphson iteration can be used to solve a non-linear system of equations. The iteration scheme for multiple dimensions is given by:

$$x^{(k+1)} = x^k - J\left(x^k\right)^{-1} F\left(x^k\right) \tag{19}$$

Table 2: Node types for an integrated energy network, specified per energy carrier. New node types are shown in bold. The last column shows the notation for the set of node types, which are subsets of the set of nodes in the graph.

Network	Node type	Specified parameters	Unknown parameters	Number of nodes
Gas	reference node	p	q	$\lvert\mathcal{V}_R^g\rvert$
	load node	q	p	$\lvert\mathcal{V}_L^g\rvert$
	slack node		p, q	$\lvert\mathcal{V}_S^g\rvert$
	reference load node	p, q		$\lvert\mathcal{V}_{RL}^g\rvert$
Electricity	slack bus	$\lvert V\rvert$, δ	P, Q	$\lvert\mathcal{V}_S^e\rvert$
	generator bus (PV-node)	P, $\lvert V\rvert$	Q, δ	$\lvert\mathcal{V}_G^e\rvert$
	load bus (PQ-node)	P, Q	$\lvert V\rvert$, δ	$\lvert\mathcal{V}_L^e\rvert$
	PVδ-node	P, $\lvert V\rvert$, δ	Q	$\lvert\mathcal{V}_{PV\delta}^e\rvert$
	QVδ-node	Q, $\lvert V\rvert$, δ	P	$\lvert\mathcal{V}_{QV\delta}^e\rvert$
	PQVδ-node	P, Q, $\lvert V\rvert$, δ		$\lvert\mathcal{V}_{PQV\delta}^e\rvert$
	PQV-node	P, Q, $\lvert V\rvert$	δ	$\lvert\mathcal{V}_{PQV}^e\rvert$
Heat	source reference slack node	T^s, h	T^r, T^o, φ, $\dot{m}$	$\lvert\mathcal{V}_{RS}^h\rvert$
	source node	T^o, φ	T^r, T^s, h, $\dot{m}$	$\lvert\mathcal{V}_S^h\rvert$
	load node	T^o, φ	T^r, T^s, h, $\dot{m}$	$\lvert\mathcal{V}_L^h\rvert$
	junction node	$m = 0$	T^r, T^s, h	$\lvert\mathcal{V}_J^h\rvert$
	source reference node	T^o, φ, h	T^r, T^s, m	$\lvert\mathcal{V}_{SR}^h\rvert$
	source temperature node	T^o, T^s, φ	T^r, h, m	$\lvert\mathcal{V}_{ST}^h\rvert$
	load reference node	T^o, φ, h	T^r, T^s, m	$\lvert\mathcal{V}_{LR}^h\rvert$
	reference node	$m = 0$, h	T^r, T^s	$\lvert\mathcal{V}_R^h\rvert$

with k the iteration and $J(x)$ the Jacobian matrix. Due to the choice for the heterogeneous coupling node connected with homogeneous dummy links, the Jacobian matrix of the integrated system of equations (18) is of the form

$$J(x) = \begin{pmatrix} J_{gg} & J_{ge} & J_{gh} & J_{gc} \\ J_{eg} & J_{ee} & J_{eh} & J_{ec} \\ J_{hg} & J_{he} & J_{hh} & J_{hc} \\ J_{cg} & J_{ce} & J_{ch} & J_{cc} \end{pmatrix} = \begin{pmatrix} J_{gg} & 0 & 0 & J_{gc} \\ 0 & J_{ee} & 0 & J_{ec} \\ 0 & 0 & J_{hh} & J_{hc} \\ 0 & 0 & J_{ch} & J_{cc} \end{pmatrix} \tag{20}$$

where the submatrices are defined as

$$J_{\alpha\beta} := \frac{\partial F^\alpha}{\partial x^\beta} \quad \text{with} \quad \alpha, \beta \in \{g, e, h, c\} \tag{21}$$

Since the coupling parameters, except possibly $T^{o,c}$, are assumed unknown, the coupling generally introduces more variables than equations. The submatrix J_{cc} is then not square, having more columns than rows. Subsequently, as the additional boundary conditions are imposed in the single-carrier parts, the submatrices J_{gg}, J_{ee}, and J_{hh} will also not be square, having more rows than

columns. This means we will solve the system as a whole, since solving the system blockwise is not possible.

However, if the (output) energy flows of the coupling components are known, the system becomes decoupled. The required additional boundary conditions can be imposed on the coupling variables by assuming (some of) them known. Imposing these boundary condition such that a (unique) solution exists means that J_{cc} is square. Furthermore, if all the heat powers are assumed known, the heat equation can be replaced with an equation $\varphi^c - (\varphi^c)^{\text{known}} = 0$, such that $J_{ch} = 0$. Then the coupling part can be solved for x^g, independent of the single-carrier parts. The coupling variables can then be substituted into the boundary conditions of the single-carrier networks, which can then be solved independent of each other.

4 Case studies

To validate and illustrate the proposed model framework, we consider a small integrated energy system, based on a case study by Shabanpour-Haghighi and Seifi [2015]. Ayele et al. [2018] considered an adapted version of this case study, using an extended energy hub approach. For comparison, we consider two different ways of coupling the single-carrier networks, one similar to Shabanpour-Haghighi and Seifi [2015] and the other similar to Ayele et al. [2018]. Figure 4 shows the graph representation for both cases. The single-carrier networks consist of three nodes each. Gas node 0^g is assumed to be connected to the national gas grid, such that this node will provide the energy for the rest of the integrated energy system. Coupling occurs at node 0 and node 2 of each network, whereas node 1 of each network is a sink. There is a compressor directly after node 1^g on the link to node 2^g in the gas network.

The choice of node types in the integrated network determines if the system is solvable. For both case studies we derive a condition such that the system has equal number of equations and variables. We consider a set of node types, per case, for which the system is (uniquely) solvable.

For both cases we use the same models for the single-carrier parts. In the gas network, links $(0^g, 1^g)$ and $(0^g, 2^g)$ represent a basic pipeline with

$$q_k = C_k \text{sign}\left(p_i^2 - p_j^2\right) \sqrt{\left|p_i^2 - p_j^2\right|} \tag{22}$$

where q_k is the gas flow in standard m^3/s and p_i is the nodal pressure in Pa. C_k is the pipe constant of pipe k given by [Osiadacz, 1987]:

$$C_k = \pi \frac{T_n}{p_n} \sqrt{\frac{R_{s,air}}{16}} \sqrt{\frac{D_k^5}{f_k L_k Z T S}} \tag{23}$$

with T_n standard temperature in K, p_n standard pressure, $R_{s,air}$ the specific gas constant of air, D_k the inner diameter of the pipe in m, L_k the length of the pipe in m, Z the gas compressibility factor, S the relative density of gas to air, and f_k the Darcy friction factor of the pipeline. The friction factor is determined from the implicit Colebrook equation for the turbulent regime:

$$\frac{1}{f_k} = -2 \log_{10}\left(\frac{\epsilon_k}{3.7 D_k} + \frac{2.51}{\text{Re}\sqrt{f_k}}\right) \tag{24}$$

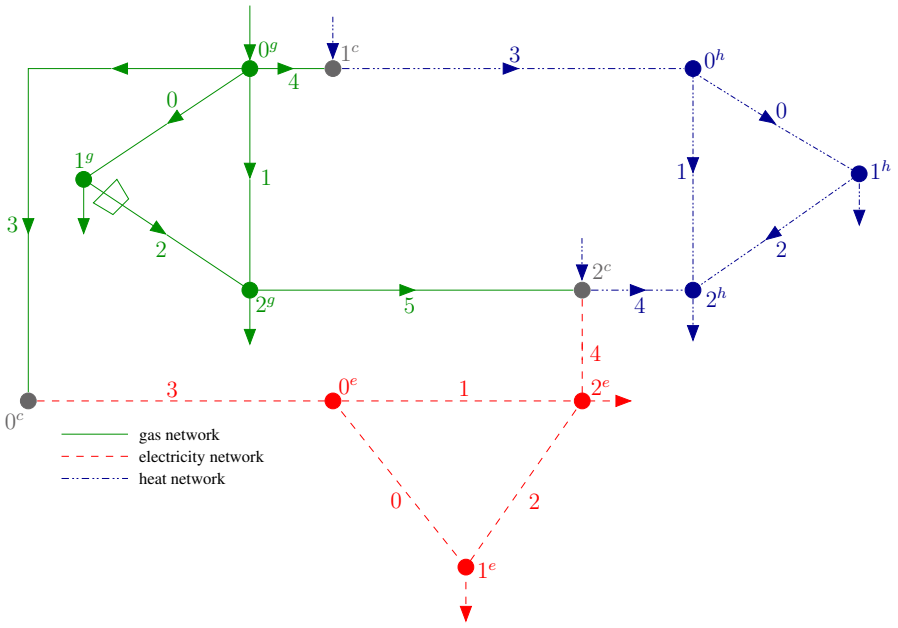

(a) Case 1

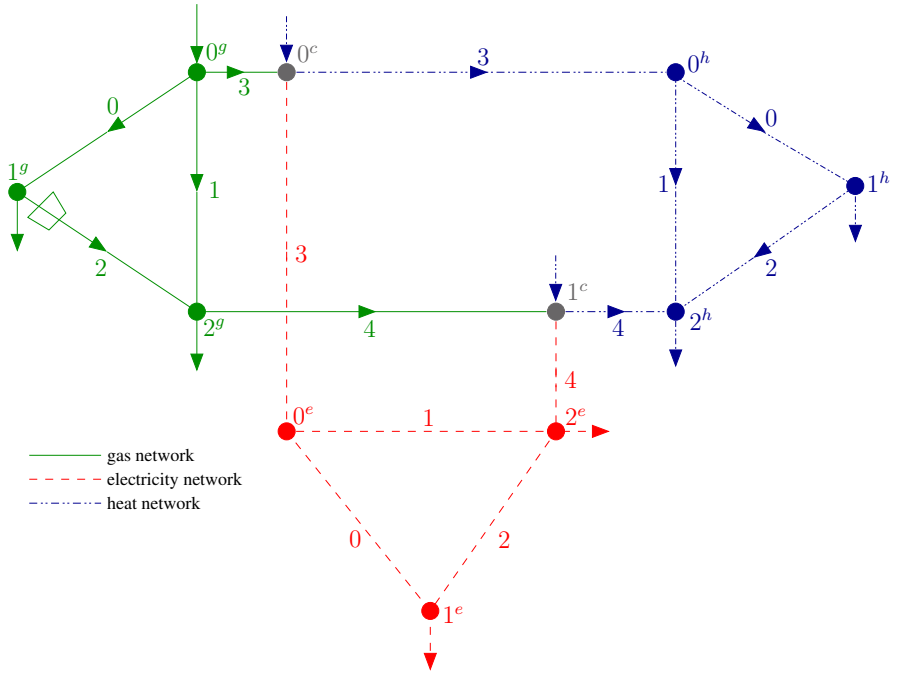

(b) Case 2

Figure 4: Network topology of the two case studies; (a) case 1 for comparison with Shabanpour-Haghighi and Seifi [2015]; (b) case 2 for comparison with Ayele et al. [2018]. In case 1 (a) node 0^g is connected to a gas-fired generator, represented by node 0^c, and to a gas-boiler, represented by node 1^c. In case 2 (b), these two components are modeled by one energy hub, represented by node 0^c. Similarly, in case 1 (a) node 2^c represents a CHP, whereas in case 2 (b) node 1^c represents an energy hub.

with ϵ_k the pipe roughness in m and Re the Reynolds number given by:

$$\mathrm{Re} = \frac{4q}{\pi D \nu} \tag{25}$$

with ν the kinematic viscosity in m^2/s. Substituting $T_n = 273.15\mathrm{K}$, $p_n = 1.01325 \cdot 10^5 \mathrm{Pa}$, and rescaling gives

$$C_k = 1.2913 \cdot 10^{-2} \sqrt{\frac{D_k^5}{f_k L_k Z T S}} \tag{26}$$

with D_k in mm and L_k in km. Taking p in bar in equation (22) then gives q_k is in standard m^3/h.

Link $(1^g, 2^g)$ represents a basic pipeline with a compressor connected at the beginning of the pipe, such that

$$q_k = C_k \mathrm{sign}\left(p_i^2 - p_j^2\right) \sqrt{\left|(Hp_i)^2 - p_j^2\right|} \tag{27}$$

with C_k given by equation (26), and $H = \frac{p_{\mathrm{out}}}{p_{\mathrm{in}}}$ the compression ratio.

We use the nodal formulation, and only use the equations for nodes where the injected gas flow is known, that is only load nodes and reference load nodes. The system of equations for the gas part is then given by

$$F^g\left(x^g\right) = A^{g\prime} q - q^{\mathrm{inj}\prime} = 0 \quad \text{with} \quad x^g = p \tag{28}$$

with $A^{g\prime}$ the $(|\mathcal{V}_L^g| + |\mathcal{V}_{RL}^g|) \times |\mathcal{E}^g|$ reduced incidence matrix, $q^{\mathrm{inj}\prime}$ the reduced vector of injected flows, and q_k is given by the link equation (22) for non-dummy links. This reduced system consist of $|\mathcal{V}_L^g| + |\mathcal{V}_{RL}^g|$ equations and $|\mathcal{V}_L^g| + |\mathcal{V}_S^g|$ variables.

In the power grid, all (non-dummy) links are represented by a short line model [Schavemaker and Van der Sluis, 2008], such that:

$$I_{ij} = y_{ij}\left(V_i - V_j\right) \tag{29}$$

where $y_{ij} = g_{ij} + \iota b_{ij}$ is the admittance of the line, with $y_{ij} = y_{ji}$. Substituting the link equation (29) in the complex power equation leads to

$$\begin{aligned} P_{ij} &= \begin{cases} g_{ij}|V_i|^2 - |V_i||V_j|\left(g_{ij}\cos\delta_{ij} + b_{ij}\sin\delta_{ij}\right) & \text{for non-dummy links} \\ P_k & \text{for dummy links} \\ 0 & \text{otherwise} \end{cases} \\ Q_{ij} &= \begin{cases} -b_{ij}|V_i|^2 - |V_i||V_j|\left(g_{ij}\sin\delta_{ij} - b_{ij}\cos\delta_{ij}\right) & \text{for non-dummy links} \\ Q_k & \text{for dummy links} \\ 0 & \text{otherwise} \end{cases} \end{aligned} \tag{30}$$

We use the complex power formulation, and only take the equations for the nodes where the injected active or reactive power is known. The system of equations for the electrical part is then given by:

$$F^e\left(x^e\right) = \begin{pmatrix} \sum\limits_{j,\, j\neq i} P_{ij} - P^{\mathrm{inj}\prime} \\ \sum\limits_{j,\, j\neq i} Q_{ij} - Q^{\mathrm{inj}\prime} \end{pmatrix} = 0 \quad \text{with} \quad x^e = \begin{pmatrix} \delta \\ |V| \end{pmatrix} \tag{31}$$

Here, $\sum_{j,\, j\neq i} P_{ij}$ and $\sum_{j,\, j\neq i} Q_{ij}$ are the reduced vectors with calculated injected active and reactive power respectively, $P^{\text{inj}\prime}$ and $Q^{\text{inj}\prime}$ are the reduced vectors of known injected active and reactive energy flows. This reduced system consists of $|\mathcal{V}_G^e| + 2|\mathcal{V}_L^e| + |\mathcal{V}_{PV\delta}^e| + |\mathcal{V}_{QV\delta}^e| + |\mathcal{V}_{PQV\delta}^e| + |\mathcal{V}_{PQV}^e|$ equations and $|\mathcal{V}_G^e| + 2|\mathcal{V}_L^e| + |\mathcal{V}_{PQV}^e|$ variables.

In the heat network, all (non-dummy) links represent a pipeline with a basic head loss equation [Ayele et al., 2018]:

$$h_i - h_j - K_k|m_k|m_k = 0 \tag{32}$$

with K_k the pipe constant given by:

$$K_k = \frac{8L_k f_k}{\pi^2 g \rho^2 D^5} \tag{33}$$

with D_k the inner diameter of the pipe in m, L_k the length of the pipe in m, ρ the density of the water in kg/m^3, and f_k the Darcy friction factor of the pipeline. The friction factor is determined from the implicit Colebrook equation for the turbulent regime (24). For the thermal model we consider the temperatures with respect to the ambient temperature. That is, we consider $T' := T - T^a$, with T^a the ambient temperature in °C. For notational simplicity, we drop the prime and simply denote this temperature as T. The pipeline has an exponential temperature drop for both supply and return:

$$T_k^{\text{end}} - \psi\left(m_k\right) T_k^{\text{start}} = 0 \quad \text{with} \quad \psi\left(m_k\right) := \exp\left(\frac{-\lambda_k L_k}{C_p|m_k|}\right) \tag{34}$$

where λ_k is the heat transfer coefficient of the pipe in W/(m K), and C_p is the specific heat of water in J/(kg K). For the terminal links the heat power equation is given by

$$\varphi_{i,l} = \begin{cases} C_p m_{i,l}\left(T_i^s - T_{i,l}^o\right) & \text{if node } i \text{ is a sink} \\ C_p m_{i,l}\left(T_{i,l}^o - T_i^r\right) & \text{if node } i \text{ is a source} \end{cases} \tag{35}$$

The mass flow of a terminal link l connected to node i can then be found by

$$m_{i,l} = \begin{cases} \dfrac{\varphi_{i,l}}{C_p\left(T_{i,l}^o - T_i^r\right)} & \text{if } v_i \in \mathcal{V}_S^h \cup \mathcal{V}_{SR}^h \cup \mathcal{V}_{ST}^h \\ \dfrac{\varphi_{i,l}}{C_p\left(T_i^s - T_{i,l}^o\right)} & \text{if } v_i \in \mathcal{V}_L^h \cup \mathcal{V}_{LR}^h \\ 0 & \text{if } v_i \in \mathcal{V}_J^h \cup \mathcal{V}_R^h \\ \displaystyle\sum_{\mathcal{E}^h} m^s & \text{if } v_i \in \mathcal{V}_{RS}^h \end{cases} \tag{36}$$

The equation for the source reference slack node is based on the assumption that there is only one component connected to it, and that $\varphi_{i,l}$ is unknown. Substituting the temperature drop (34) and

the components mass flow (36) in the mixing rule (13) leads to $F^{T^s} = 0$ for the supply line, with

$$F_i^{T^s} = \begin{cases} \left(\sum_{\mathcal{E}^h} m_{out}^s\right) T_i^s - \sum_j |m_{ij}|\psi_{ij} T_j^s - \sum_l \left(-m_{i,l} T_{i,l}^o\right) & \text{if } v_i \in \mathcal{V}_S^h \cup \mathcal{V}_{SR}^h \cup \mathcal{V}_{ST}^h \\ \left(\sum_{\mathcal{E}^h} m_{out}^s + \sum_l m_{i,l}\right) T_i^s - \sum_j |m_{ij}|\psi_{ij} T_j^s & \text{if } v_i \in \mathcal{V}_L^h \cup \mathcal{V}_{LR}^h \\ \left(\sum_{\mathcal{E}^h} m_{out}^s\right) T_i^s - \sum_j |m_{ij}|\psi_{ij} T_j^s & \text{if } v_i \in \mathcal{V}_J^h \cup \mathcal{V}_R^h \\ \left(\sum_{\mathcal{E}^h} m_{out}^s\right) T_i^s - \sum_j |m_{ij}|\psi_{ij} T_j^s - (-m_i T_i^o) & \text{if } v_i \in \mathcal{V}_{RS}^h \end{cases} \tag{37}$$

Similarly, the mixing rule (13) for the return temperature is then given by $F^{T^r} = 0$, with

$$F_i^{T^r} = \begin{cases} \left(\sum_{\mathcal{E}^h} m_{in}^s + \sum_l -m_{i,l}\right) T_i^r - \sum_j |m_{ij}|\psi_{ij} T_j^r & \text{if } v_i \in \mathcal{V}_S^h \cup \mathcal{V}_{SR}^h \cup \mathcal{V}_{ST}^h \\ \left(\sum_{\mathcal{E}^h} m_{in}^s\right) T_i^r - \sum_j |m_{ij}|\psi_{ij} T_j^r - \sum_l \left(m_{i,l} T_{i,l}^o\right) & \text{if } v_i \in \mathcal{V}_L^h \cup \mathcal{V}_{LR}^h \\ \left(\sum_{\mathcal{E}^h} m_{in}^s\right) T_i^r - \sum_j |m_{ij}|\psi_{ij} T_j^r & \text{if } v_i \in \mathcal{V}_J^h \cup \mathcal{V}_R^h \\ \left(\sum_{\mathcal{E}^h} m_{in}^s - m_i\right) T_i^r - \sum_j |m_{ij}|\psi_{ij} T_j^r & \text{if } v_i \in \mathcal{V}_{RS}^h \end{cases} \tag{38}$$

While for the gas network the nodal formulation is commonly used, this is not done for the heat network. The nodal formulation would make the Jacobian matrix complicated due to the dependence of edge mass flow on heads and, in turn, the dependence of the mixing rules on these edge flows. One of the commonly used formulations is the loop formulation which is for instance used by Liu et al. [2016] and Shabanpour-Haghighi and Seifi [2015]. However, this requires loops to be found in the network. Furthermore, it is common to substitute conservation of mass (10) in the heat equation (12), resulting in a 'conservation of heat'. However, this formulation is inconvenient when defining dummy links, and the interpretation for a node with multiple components is unclear. Therefore, we formulate the system based on Ayele et al. [2018] for the hydraulic part and on Abeysekera [2016] for the thermal part. Essentially, we do not reduce the size of the hydraulic part and only apply algebraic substitutions in the thermal part. The conservation of flow and the supply mixing rule are not taking into F^h for source reference slack nodes. Similarly, the head and supply temperature are not part of x^h for source reference slack nodes. The head is also not part of x^h for source reference, load reference or reference nodes. And the supply temperature is not part of x^h for source temperature nodes. The system of equations for the heat part is then given by

$$F^h\left(x^h\right) = \begin{pmatrix} A^{h\prime} m - m^{\text{inj}\prime} \\ \left(A^h\right)^T h - \text{Diag}\left(K\right) \text{Diag}\left(|m|\right) m \\ F^{T^s} \\ F^{T^r} \end{pmatrix} = 0 \quad \text{with } x^h = \begin{pmatrix} m \\ h' \\ T^{s\prime} \\ T^r \end{pmatrix} \tag{39}$$

Table 3: Values of parameters for both case studies, per network. Here, $|\cdot|_b$ denotes the base value, and p.u. stands for per unit.

Network	**Network parameters**			**Carrier parameters**				**Link**	**Link parameters**			
gas	$\lvert E^g\rvert_b$ [MW]	T_n [°C]	p_n [10^5 Pa]	GHV [10^{-2} MW/m^3]	Z [–]	S [–]	ν [10^{-6} m/s]		L [km]	D [mm]	ϵ [mm]	H [–]
	100	273.15	1.01325	1.19034	0.8	0.6106	0.288	0-1	30	150	0.05	
								0-2	30	150	0.05	
								1-2	30	150	0.05	1.3
power	$\lvert S\rvert_b$ [MW]								x [p.u.]	r [p.u.]		
	100							0-1	0.5	0.05		
								0-2	0.5	0.05		
								1-2	0.5	0.05		
heat	$\lvert\varphi\rvert_b$ [MW]	$T^{\text{ref}}_{\text{high}}$ [°C]	T^a [°C]	C_p [10^{-3} MJ K/kg]	ρ [kg/m^3]		ν [10^{-6} m/s]		L [km]	D [mm]	ϵ [mm]	λ [W K/m]
	100	130	10	4.182	960		0.294	0-1	30	150	1.23	0.2
								0-2	30	150	1.23	0.2
								1-2	30	150	1.23	0.2

with $m_i^{\text{inj}} = \sum_l m_{i,l}$, $A^{h\prime}$ the reduced incidence matrix, $m^{\text{inj}\prime}$ the reduced vector of injected flows, and $T^{s\prime}$ and $T^{r\prime}$ the reduced vector of supply and return temperatures respectively. Diag (v) is used to denote a diagonal matrix with vector v on the diagonal. This reduced system consists of $3|\mathcal{V}_S^h| + 3|\mathcal{V}_L^h| + 3|\mathcal{V}_J^h| + |\mathcal{V}_{RS}^h| + 3|\mathcal{V}_{SR}^h| + 3|\mathcal{V}_{ST}^h| + 3|\mathcal{V}_{LR}^h| + 3|\mathcal{V}_R^h| + |\mathcal{E}_{ND}^h|$ equations and $3|\mathcal{V}_S^h|+3|\mathcal{V}_L^h|+3|\mathcal{V}_J^h|+|\mathcal{V}_{RS}^h|+2|\mathcal{V}_{SR}^h|+2|\mathcal{V}_{ST}^h|+2|\mathcal{V}_{LR}^h|+2|\mathcal{V}_R^h|+|\mathcal{E}_{ND}^h|$variables. Here, $\mathcal{E}_{ND}^h$ denotes the set of non-dummy heat links in the network.

To solve the total system of equations (of the form (18)), we adopt a per unit formulation for the single-carrier networks and the coupling part. This normalization is commonly used in power grids. Appendix A gives details about the formulation for all three networks. Table 3 gives the values for the network parameters used in both cases.

4.1 Case 1

Case 1 is used for comparison with the case study of Shabanpour-Haghighi and Seifi [2015]. Node 0^c represents a gas-fired generator, node 1^c a gas boiler, and node 2^c a combined heat and power plant (CHP). For the coupling components we use the same models as Shabanpour-Haghighi and Seifi [2015]:

$$\begin{aligned} f_0^c\left(q_3, P_3\right) &= aP_3^2 + bP_3 + c + \left|d\sin\left(e\left(P^{\min} - P_3\right)\right)\right| - \text{GHV}q_3 = 0 \\ f_1^c\left(q_4, \varphi_{1^c}\right) &= \varphi_{1^c} - \eta_{GB}\text{GHV}q_4 = 0 \\ f_2^c\left(q_5, P_4, \varphi_{2^c}\right) &= P_4 + \varphi_{2^c} - \eta_{CHP}\text{GHV}q_5 = 0 \end{aligned} \tag{40}$$

with a, b, c, d, and e parameters of the gas-fired generator and $P^{\min}$ the minimum produced power, η_{GB} the efficiency of the gas boiler, and η_{CHP} of the CHP. We take $a = 0.002\,931$, $b = 1.1724$, $c = 43.965$, $d = 4.3965$, $e = 0.5$, $\eta_{GB} = 0.88$, and $\eta_{CHP} = 0.88$.

Combining the coupling equations above with the heat power equations and (optionally) with

equations for the outflow temperature gives the system of equations for the coupling part:

$$F^c\left(x^c\right) = \begin{pmatrix} P_3 - \eta_{GG}\mathrm{GHV}q_3 \\ \varphi_{1^c} - \eta_{GB}\mathrm{GHV}q_4 = 0 \\ P_4 + \varphi_{2^c} - \eta_{CHP}\mathrm{GHV}q_5 \\ \varphi_{1^c} - C_p m_3 \left(T^o_{1^c} - T^r_{0^h}\right) \\ \varphi_{2^c} - C_p m_4 \left(T^o_{2^c} - T^r_{2^h}\right) \\ T^o_{1^c} - \left(T^o_{1^c}\right)^{\text{known}} \\ T^o_{2^c} - \left(T^o_{2^c}\right)^{\text{known}} \end{pmatrix} = 0 \quad \text{with} \quad x^c = \begin{pmatrix} q_3 \\ q_4 \\ q_5 \\ P_3 \\ P_4 \\ Q_3 \\ Q_4 \\ m_3 \\ m_4 \\ \varphi_{1^c} \\ \varphi_{2^c} \\ T^o_{1^c} \\ T^o_{2^c} \end{pmatrix} \tag{41}$$

A system like this, where every coupling node has only one coupling equation f^c and a maximum of one dummy link per energy carrier, consists of $|\mathcal{V}^c_{ge}| + 2|\mathcal{V}^c_{gh,S}| + 3|\mathcal{V}^c_{gh,T}| + 2|\mathcal{V}^c_{eh,S}| + 3|\mathcal{V}^c_{eh,T}| + 2|\mathcal{V}^c_{geh,S}| + 3|\mathcal{V}^c_{geh,T}|$ equations and $3|\mathcal{V}^c_{ge}| + 4|\mathcal{V}^c_{gh}| + 5|\mathcal{V}^c_{eh}| + 6|\mathcal{V}^c_{geh}|$ variables. Here, $\mathcal{V}^c_{\alpha\beta}$ and $\mathcal{V}^c_{\alpha\beta\gamma}$ denote the set of coupling nodes which are linked to networks with energy carriers α, β, $\gamma \in \{g, e, h\}$. The subscript S denotes a *standard coupling node*, with unknown outflow temperature $T^{o,c}$, while the subscript T indicates a *temperature coupling node* with known outflow temperature. For the latter, an equation $T^{o,c} - \left(T^{o,c}\right)^{\text{known}} = 0$ is added to the system of equations.

Combining the systems of equations (28), (31), (39), and (41), results in a total system of equations of the form (18). This system has the same number of equations as variables, that is $|F\left(x\right)| = |x|$ if

$$\begin{aligned} |\mathcal{V}^g_{RL}| + |\mathcal{V}^e_{PV\delta}| + |\mathcal{V}^e_{QV\delta}| + 2|\mathcal{V}^e_{PQV\delta}| + |\mathcal{V}^e_{PQV}| + |\mathcal{V}^h_{SR}| + |\mathcal{V}^h_{ST}| + |\mathcal{V}^h_{LR}| + |\mathcal{V}^h_{R}| = & |\mathcal{V}^g_{S}| + 2|\mathcal{V}^c_{ge}| 2|\mathcal{V}^c_{gh,S}| + |\mathcal{V}^c_{gh,T}| + 3|\mathcal{V}^c_{eh,S}| \\ & + 2|\mathcal{V}^c_{eh,T}| + 4|\mathcal{V}^c_{geh,S}| + 3|\mathcal{V}^c_{geh,T}| \end{aligned} \tag{42}$$

Assuming the node types in the single-carrier were such that they were solvable, these couplings require 8 additional boundary conditions to be added. We will consider the set of nodes types shown in Table 4a. The power grid and the heat network do not have any external inflow; all the energy is provided by the gas network. This means that that node 0^h is a junction. Node 0^e has a heat pump connected to it in the case study by Shabanpour-Haghighi and Seifi [2015], such that the total injected active power for node 0^e is equal to the power supplied to that heat pump. Both these nodes will be taken as reference nodes, which means that 0^e is a $PQV\delta$-node and node 0^h is a reference node. We assume the outflow temperature of the gas-boiler and the CHP to be known, as is done for any heat source or sink. Then, three more additional boundary conditions are needed; one is imposed on node 1^g, one on node 2^e, and the last on node 2^h.

Table 4: Node types for both cases. The x and F column show the amount of variables and functions the node contributes to the system. For the total system of equations, all non-dummy heat links contribute one entry to x and one to F.

(a) Case 1.

Node	Type	x	F
0^g	ref.	0	0
1^g	load	1	1
2^g	ref. load	0	1
0^e	PQVδ	0	2
1^e	load	2	2
2^e	PQV	1	2
0^h	ref.	2	3
1^h	load	3	3
2^h	load ref.	2	3
0^c	ge	3	1
1^c	gh temp.	4	3
2^c	geh temp.	6	3
Total		27	27

(b) Case 2.

Node	Type	x	F
0^g	ref.	0	0
1^g	load	1	1
2^g	load	1	1
0^e	PQVδ	0	2
1^e	load	2	2
2^e	PQV	1	2
0^h	ref.	2	3
1^h	load	3	3
2^h	load	3	3
0^c	geh temp.	6	4
1^c	geh temp.	6	4
Total		28	28

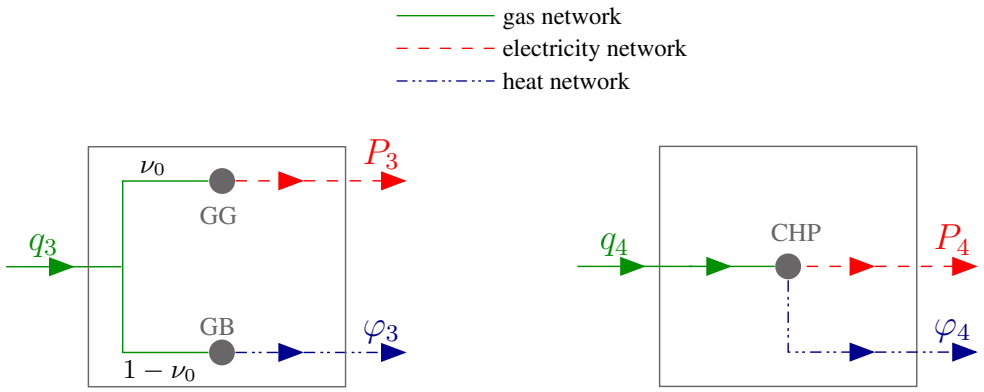

(a) Energy hub 0 (b) Energy hub 1

Figure 5: Schematic representation of the energy hubs. (a) shows energy hub 0 consisting of a gas-fired generator (GG) and a gas boiler (GB). ν_0 denotes the fraction of q_3 provided to the generator. (b) shows energy hub 1 consisting of a CHP. Here, q is gas flow, P is active power, and φ is heat power. Energy hubs 0 and 1 are represented by nodes 0^c and q^c in Figure 4b respectively.

4.2 Case 2

Case 2 is used for comparison with the case study of Ayele et al. [2018]. Both nodes 0^c and 1^c represent an energy hub, called energy hub 0 and energy hub 1 respectively. Energy hub 0 consists of a gas-fired generator and a gas-boiler, energy hub 1 consists only of a CHP. Figure 5 shows a schematic representation of both energy hubs.

For both energy hubs we use a coupling matrix C as suggested by Geidl and Andersson [2007]. The entry $c_{\alpha\beta}$ of C gives the conversion factor from energy carrier α to carrier β. Based on the schematic representation of the energy hubs we find:

$$\begin{aligned}
\begin{pmatrix} \mathrm{GHV} q_3 \\ P_3 \\ \varphi_{0^c} \end{pmatrix}_{\text{out}} &= \begin{pmatrix} 0 & 0 & 0 \\ \eta_{GG}\nu_0 & 0 & 0 \\ \eta_{GB}\,(1-\nu_0) & 0 & 0 \end{pmatrix} \begin{pmatrix} \mathrm{GHV} q_3 \\ P_3 \\ \varphi_{0^c} \end{pmatrix}_{\text{in}} := C_0 \begin{pmatrix} \mathrm{GHV} q_3 \\ P_3 \\ \varphi_3 \end{pmatrix}_{\text{in}} \\
\begin{pmatrix} \mathrm{GHV} q_4 \\ P_4 \\ \varphi_{1^c} \end{pmatrix}_{\text{out}} &= \begin{pmatrix} 0 & 0 & 0 \\ \eta_{CHP}\nu_1 & 0 & 0 \\ \eta_{CHP}\,(1-\nu_1) & 0 & 0 \end{pmatrix} \begin{pmatrix} \mathrm{GHV} q_4 \\ P_4 \\ \varphi_{1^c} \end{pmatrix}_{\text{in}} := C_1 \begin{pmatrix} \mathrm{GHV} q_4 \\ P_4 \\ \varphi_{1^c} \end{pmatrix}_{\text{in}}
\end{aligned} \tag{43}$$

The coupling matrix itself allows for bidirectional flow. If for instance $c_{eg}, c_{hg} \neq 0$, these hubs could also convert power and heat back to gas. For this case, unidirectional flow is assumed, since the physical components can only convert gas to power and heat. The coupling equations are then given by:

$$\begin{aligned}
\begin{pmatrix} P_3 \\ \varphi_{0^c} \end{pmatrix} &= \begin{pmatrix} \eta_{GG}\nu_0 \\ \eta_{GB}\,(1-\nu_0) \end{pmatrix} (\mathrm{GHV} q_3) \\
\begin{pmatrix} P_4 \\ \varphi_{1^c} \end{pmatrix} &= \begin{pmatrix} \eta_{CHP}\nu_1 \\ \eta_{CHP}\,(1-\nu_1) \end{pmatrix} (\mathrm{GHV} q_4)
\end{aligned} \tag{44}$$

We take $\eta_{GG} = 0.45$, $\eta_{GB} = 0.88$, $\eta_{CHP} = 0.88$, $\nu_0 \approx 0.775\,05$, and $\nu_1 \approx 0.266\,34$

The system of equations for the coupling part is then given by

$$F^c\left(x^c\right) = \begin{pmatrix} P_3 - c^0_{ge}\mathrm{GHV}q_3 \\ \varphi_{0^c} - c^0_{gh}\mathrm{GHV}q_3 \\ P_4 - c^1_{ge}\mathrm{GHV}q_4 \\ \varphi_{1^c} - c^1_{gh}\mathrm{GHV}q_4 \\ \varphi_{0^c} - C_p m_3 \left(T^o_{0^c} - T^r_{0^h}\right) \\ \varphi_{1^c} - C_p m_4 \left(T^o_{1^c} - T^r_{1^h}\right) \\ T^o_{0^c} - \left(T^o_{0^c}\right)^{\text{known}} \\ T^o_{1^c} - \left(T^o_{1^c}\right)^{\text{known}} \end{pmatrix} = 0 \quad \text{with} \quad x^c = \begin{pmatrix} q_3 \\ q_4 \\ P_3 \\ P_4 \\ Q_3 \\ Q_4 \\ m_3 \\ m_4 \\ \varphi_{0^c} \\ \varphi_{0^c} \\ T^o_{0^c} \\ T^o_{1^c} \end{pmatrix} \tag{45}$$

A system like this, where every coupling node has an energy hub matrix equation as coupling equation, and a maximum of one dummy link per energy carrier, consists of $|E^{out}_{ge}||\mathcal{V}^c_{ge}|+\left(|E^{out}_{gh,S}|+1\right)|\mathcal{V}^c_{gh,S}|+\left(|E^{out}_{gh,T}|+2\right)|\mathcal{V}^c_{gh,T}|+\left(|E^{out}_{eh,S}|+1\right)|\mathcal{V}^c_{eh,S}|+\left(|E^{out}_{eh,T}|+2\right)|\mathcal{V}^c_{eh,T}|+\left(|E^{out}_{geh,S}|+1\right)|\mathcal{V}^c_{geh,S}|+\left(|E^{out}_{geh,T}|+2\right)|\mathcal{V}^c_{geh,T}|$ equations and $3|\mathcal{V}^c_{ge}|+4|\mathcal{V}^c_{gh}|+5|\mathcal{V}^c_{eh}|+6|\mathcal{V}^c_{geh}|$ variables.

Combining the systems of equations (28), (31), (39), and (45), results in a total system of equations of the form (18). Assuming the node types in the single-carrier networks were such that, before coupling, those networks were solvable, these couplings require 6 additional boundary conditions. We will consider the set of node types shown in Table 4b. Similar to case 1, 0^e is a $PQV\delta$-node, 1^e a PQV-node, and node 0^h is a reference node. We assume the outflow temperature of both energy hubs to be known, as is done for any heat source or sink.

Compared with case 1, 6 additional boundary conditions are needed instead of 8. This is because the energy hub concept specifies the ratio between the input powers for hub 0, and the output powers for hub 1. Instead of imposing 2 additional boundary conditions in case 1, we could also add 2 equations in accordance with the energy hubs. The first would give the ratio between q_3 and q_4, the second between P_4 and φ_4. Conversely, if ν_0 and ν_1 are unknown, or functions of the in- or output power, the ratio between the powers in the energy hub becomes unknown. Then, a total of 8 additional boundary conditions would be required in case 2.

4.3 Results

We use a basic Newton-Raphson method to solve the system of equations for both cases. With a tolerance of 10^{-6} p.u. the method converged in 4 iterations for case 1 and 5 iterations for case 2.

Table 5: Results for the gas network, (a) for case 1 with node types set 1, and (b) for Shabanpour-Haghighi and Seifi [2015].

Node	p [bar]		q^{inj} $\left[10^3 \,\text{standard}\,\text{m}^3/\text{h}\right]$		**Link**	q $\left[10^3 \,\text{standard}\,\text{m}^3/\text{h}\right]$	
	(a)	(b)	(a)	(b)		(a)	(b)
0	50	50.0000	-46.715	-47.1083	0-1	18.2327	29.8308
1	29.1021	40.8160	10.8649	10	0-2	16.4078	4.8098
2	34.0770	49.7827	20	20	1-2	7.3678	18.9658

Table 6: Results for the electrical network, (a) for case 1 with node types set 1, and (b) for Shabanpour-Haghighi and Seifi [2015].

Node	$\lvert V\rvert$ [p.u.]		δ [°]		S^{inj} [MW]	
	(a)	(b)	(a)	(b)	(a)	(b)
0	1.06	1.0600	0	0	0.1451+0ι	0+0ι
1	0.9801	0.9800	-6.9888	-7.0219	30+15ι	30.0000+15.0000ι
2	1	1.000	-6.048	-6.1156	30.1360+15ι	30.1360 +15.0000ι
Link	S_{ij} [MW]		S_{ji} [MW]		S_{ij}^{loss} [MW]	
	(a)	(b)	(a)	(b)	(a)	(b)
0-1	26.8615+15.8007ι	26.9806+15.8106ι	-26.4293-11.4789ι	-26.5454-11.4588ι	0.4322+4.3218ι	0.4352+4.3518ι
0-2	23.4916+11.5508ι	23.7405+11.5524ι	-23.1867-8.5013ι	-23.4303-8.4505ι	0.3049+3.0495ι	0.3102+3.1019ι
1-2	-3.5707-3.5211ι	-3.4546-3.5412ι	3.5838+3.6520ι	3.4673+3.6686ι	0.0131+0.1309ι	0.0127+0.1274ι
Total					0.7502+7.5022ι	0.7581+7.5811ι

Table 7: Results for hydraulic part of the heat network, (a) for case 1 with node types set 1, and (b) for Shabanpour-Haghighi and Seifi [2015].

Node	h [m]		m^{inj} [kg/s]		**Link**	m [kg/s]	
	(a)	(b)	(a)	(b)		(a)	(b)
0	5517	-	0	-	0-1	64.6877	64.6943
1	224.9319	-	121.2256	-	0-2	31.4083	31.4533
2	4268.1087	-	65.0282	-	1-2	-56.5379	-56.5335

Table 8: Results for the thermal part of the heat network, (a) for case 1 with node types set 1, and (b) for Shabanpour-Haghighi and Seifi [2015].

Node	T^s [°C]		T^r [°C]		φ [MW]		**Link**	φ^{loss} [MW]	
	(a)	(b)	(a)	(b)	(a)	(b)		(a)	(b)
0	120	120	48.6800	48.6805	0	0	0-1	0.8901	0.8901
1	119.0382	119.0370	50	50	35	35	0-2	0.8770	0.8770
2	123.5435	123.5410	49.5339	49.5339	20	20	1-2	0.9097	0.9097
Total								2.6768	2.6768

Table 9: Results for the coupling network, (a) for case 1 with node types set 1, and (b) for Shabanpour-Haghighi and Seifi [2015].

Node	q $[10^3\,\text{standard}\,\text{m}^3/\text{h}]$		P [MW]		Q [VAr]		m [kg/s]		φ [MW]		T^o [°C]	
	(a)	(b)	(a)	(b)	(a)	(b)	(a)	(b)	(a)	(b)	(a)	(b)
0 (GG)	9.3382	9.4501	50.4982	50.8662	27.3515	27.3630	-	-	-	-	-	-
1 (GB)	2.7363	3.0177	-	-	-	-	96.0960	-	28.6616	28.6768	120	-
2 (CHP)	3.7756	3.3581	10.5331	10.1730	10.1507	10.2181	90.1578	-	29.0152	29	126.4891	-

Tables 5-9 show the results for case 1 and the results found by Shabanpour-Haghighi and Seifi [2015]. There are some differences in the solution, which could be due to differences in implementations or models. For the gas network, it seems that the flows obtained by plugging in the pressures presented by Shabanpour-Haghighi and Seifi [2015] in their flow equation, do match their presented gas pipe flows. The ratio between their presented gas flows and the flows found by substituting the pressures in the flow equation (22), with pipe constant (26), seems to be a factor $\ln 10$. For the heat network, the differences could also partly be due to the model choice. Shabanpour-Haghighi and Seifi [2015] use a loop formulation and conservation of heat in the nodes, whereas we use a combined nodal-loop formulation and conservation of mass in the nodes. Moreover, we do not consider the heat boiler connected between node 2^g and node 2^h, which means that all the heat is supplied by the CHP, which only has one outflow temperature. Finally, we do not model the heat pumps, but take those as constant electrical demands for node 0^e and 2^e.

Tables 10-14 show the results for case 2 and the results found by Ayele et al. [2018]. They do not model the gas network explicitly, so Table 10 only includes our solution. Again, there are some small differences in the solution, which could be due to differences in implementations or in models. First, we use a slightly different formulation for hydraulic-thermal model of the heat network than Ayele et al. [2018]. Second, Ayele et al. [2018] use a different model for loads and sources. That is, they use the difference between nodal supply and return temperature in the heat power equation, whereas we use the difference between a component's outflow temperature and the nodal supply or return temperature. This could explain the difference in the nodal temperatures. Finally, they use a different model for the temperature drop in a pipeline, which could explain the differences in mass flow and in the heat power loss.

Table 10: Results for the gas network, (a) for case 2 with node types set 1, and (b) for Ayele et al. [2018].

Node	p [bar]		q^{inj} $\left[10^3 \,\text{standard}\,\text{m}^3/\text{h}\right]$		**Link**	q $\left[10^3 \,\text{standard}\,\text{m}^3/\text{h}\right]$	
	(a)	(b)	(a)	(b)		(a)	(b)
0	50	-	-46.8044	-	0-1	18.2327	-
1	29.1021	-	10.8649	-	0-2	16.4078	-
2	34.077	-	20	-	1-2	7.3678	-

Table 11: Results for the electrical network, (a) for case 2 with node types set 1, and (b) for Ayele et al. [2018].

Node	$\lvert V\rvert$ [p.u.]		δ [°]		S^{inj} [MW]	
	(a)	(b)	(a)	(b)	(a)	(b)
0	1.06	1.06	0	0	0.1451+0$\imath$	0.1451+0$\imath$
1	0.98008	0.98005	-6.9888	-7.0219	30+15$\imath$	30.0000+15.0000$\imath$
2	1	1	-6.1139	-6.048	30.1360 +15$\imath$	30.1360 +15.0000$\imath$
Link	S_{ij} [MW]		S_{ji} [MW]		S_{ij}^{loss} [MW]	
	(a)	(b)	(a)	(b)	(a)	(b)
0-1	26.8615+15.8007$\imath$	26.981+15.811$\imath$	-26.4293-11.4789$\imath$	-	0.4322 +4.3218$\imath$	0.4352+4.3518$\imath$
0-2	23.4916+11.5508 $\imath$	23.740+11.552$\imath$	-23.1867-8.5013$\imath$	-	0.3049+3.0495$\imath$	0.3102+3.1019$\imath$
1-2	-3.5707-3.5211$\imath$	-3.4546-3.5412$\imath$	3.5838+3.652$\imath$	-	0.0131+0.1309$\imath$	0.0127+0.1274$\imath$
Total					0.7502+7.5022$\imath$	0.7581+7.5811$\imath$

Table 12: Results for hydraulic part of the heat network, (a) for case 2 with node types set 1, and (b) for Ayele et al. [2018].

Node	h [m]		m^{inj} [kg/s]		**Link**	m [kg/s]	
	(a)	(b)	(a)	(b)		(a)	(b)
0	5517	5517	0	-	0-1	64.6877	65.962
1	224.9319	10.666	121.2256	-	0-2	31.4083	29.893
2	4268.1087	4383.8	65.0282	-	1-2	-56.5379	-58.778

Table 13: Results for the thermal part of the heat network, (a) for case 2 with node types set 1, and (b) for Ayele et al. [2018].

Node	T^s [°C]		T^r [°C]		φ [MW]		**Link**	φ^{loss} [MW]	
	(a)	(b)	(a)	(b)	(a)	(b)		(a)	(b)
0	120	120	48.6801	48.536	0	0	0-1	0.8901	0.8903
1	119.0382	117.09	50	50	35	35	0-2	0.877	0.8731
2	123.5435	123.541	49.5339	49.035	20	20	1-2	0.9097	0.8839
Total								2.6768	2.6473

Table 14: Results for the coupling network, (a) for case 2 with node types set 1, and (b) for Ayele et al. [2018].

Node	q $[10^3\,\text{standard}\,\text{m}^3/\text{h}]$		P [MW]		Q [VAr]		m [kg/s]		φ [MW]		T^o [°C]	
	(a)	(b)	(a)	(b)	(a)	(b)	(a)	(b)	(a)	(b)	(a)	(b)
0	12.1639	-	50.4982	50.8662	27.3515	27.3630	96.096	-	28.6616	28.647	120	-
1	3.7756	-	10.5331	10.173	10.1507	10.2181	90.1578	-	29.0152	29	126.4891	-

5 Conclusion

We developed a general model framework for steady-state load flow analysis of multi-carrier energy systems (MES), consisting of gas, heat, and electricity. The framework is based on connecting single-carrier networks to heterogeneous coupling nodes, using dummy links, to make an integrated energy network. The coupling node is any node that has in- or outflow of one or more energy carriers. It allows bidirectional flow, and can represent a variety of couplings, such as a single converter component, an energy hub, or a complete heterogeneous network. Having the coupling node represent a complete heterogeneous network could lead to a hierarchical approach.

We analyzed the resulting graph-representation and the corresponding load flow models, which introduced new node types for the single-carrier parts. Using these new node types, a system of non-linear equations is formulated, in which all single-carrier networks are independent of each other. This approach gives a sparse Jacobian matrix with a distinct structure, in which the sub-matrices are not necessarily square. Moreover, we found a necessary condition for a solution to exist, in terms of the number of node types. However, care must be taken when choosing the node types and the locations of the coupling nodes in the graph. Certain combinations of node types can result in unsolvable systems. For instance, some subnetworks can become overdetermined while others are underdetermined. Our systematic approach to the graph representation of MES, and corresponding formulation of system of equations, provides insight into which coupling nodes or boundary conditions lead to an unsolvable system.

Using our proposed framework, we modeled two small MES consisting of gas, power, and heat. The two cases have similar single-carrier networks, but use different coupling models. This showed that the framework can be applied to a general system, as opposed to the case specific approaches, and that it can be used with different coupling models, as opposed to the energy hub concept. Moreover, it allows to determine both energy flows through the network and network state parameters. Finally, the framework provides a graph representation of general MES. Hence, it could be used to perform steady-state load flow analysis on cases of realistic size. Therefore, our proposed graph-based framework for steady-state load flow analysis of MES extends and generalizes the currently available models.

A Per unit system

The normalization of quantities is common practice for power grids. This is called the per unit system, see for instance Schavemaker and Van der Sluis [2008]. Ayele et al. [2018] extended this system to the heat network, to have consistency throughout the MES. Further extending this notion, we adopt a per unit system in the gas network as well. The total system of equations (18) is then solved using the per unit values. In the case studies, the pipe constants for gas (26) and heat (33) are determined using the actual values.

The per unit value of a quantity x is defined as:

$$x_{\text{p.u.}} = \frac{x_{\text{a}}}{x_{\text{b}}} \tag{46}$$

where x_{a} is the actual value and x_{b} is the base value. The per unit value is dimensionless, but is generally given dimension p.u..

For a power grid, $|V|_{\text{b}}$ and $|S|_{\text{b}}$ are usually given. The other base values are then determined by:

$$\begin{aligned} |I|_{\text{b}} &= \begin{cases} \dfrac{|S|_{\text{b}}}{|V|_{\text{b}}} & \text{for single-phase flow} \\ \dfrac{|S|_{\text{b}}}{\sqrt{3}|V|_{\text{b}}} & \text{for three-phase flow} \end{cases} \\ |y|_{\text{b}} &= \frac{|S|_{\text{b}}}{|V|_{\text{b}}^2} \end{aligned} \tag{47}$$

For the heat network, the same base value is used for the heat power as for the complex power, such that $\varphi_{\text{b}} = |S|_{\text{b}}$. Then, Ayele et al. [2018] introduce a a high and a low reference temperature, denoted by $T_{\text{ref}}^{\text{high}}$ and $T_{\text{ref}}^{\text{low}}$ respectively. The difference between the two is used as base value for a temperature difference $\Delta T := T^1 - T^2$, that is

$$\Delta T_{\text{b}} = T_{\text{ref}}^{\text{high}} - T_{\text{ref}}^{\text{low}} \tag{48}$$

such that the per unit temperature is determined as

$$T_{\text{p.u.}} = \frac{T_{\text{a}} - T_{\text{ref}}^{\text{low}}}{T_{\text{ref}}^{\text{high}} - T_{\text{ref}}^{\text{low}}} \tag{49}$$

Note that it then holds that $\Delta T_{\text{p.u}} = T_{\text{p.u}}^1 - T_{\text{p.u}}^2$. However, we use the temperature with respect to the ambient temperature, that is, we consider $T' = T - T^a$. In order for $T'_{\text{p.u.}} = T_{\text{p.u.}} - T_{\text{p.u.}}^a$, we find that $T_{\text{ref}}^{\text{low}} = 0$. Using the head loss equation (32) and the heat equation (35), the base values for the head h, mass flow m, and pipe length L are given by:

$$\begin{aligned} m_{\text{b}} &= \frac{\varphi_{\text{b}}}{C_p \Delta T_{\text{b}}} \\ h_{\text{b}} &= m_{\text{b}}^2 \\ L_{\text{b}} &= m_{\text{b}} \end{aligned} \tag{50}$$

Another option is to choose, for instance, φ_b and m_b, and then determine ΔT_b and L_b.

For the gas network, the same base value is used for the energy as is used for the heat power and the complex power, such that $E^g_\mathrm{b} = |S|_\mathrm{b}$, with the gas power given by:

$$E^g_\mathrm{a} = \mathrm{GHV} q_\mathrm{a} \tag{51}$$

Defining the per unit gas power as:

$$E^g_\mathrm{p.u.} = q_\mathrm{p.u.} \tag{52}$$

gives the base values for the volume flow q and pressure p as:

$$\begin{aligned} q_\mathrm{b} &= \frac{E^g_\mathrm{b}}{\mathrm{GHV}} \\ p_\mathrm{b} &= q_\mathrm{b} \end{aligned} \tag{53}$$

References

Pierluigi Mancarella. MES (multi-energy systems): An overview of concepts and evaluation models. *Energy*, 65:1–17, jul 2014. doi: 10.1016/j.energy.2013.10.041.

Martin Geidl and Göran Andersson. Optimal Power Flow of Multiple Energy Carriers. *IEEE Transactions on Power Systems*, 22(1):145–155, 2007. ISSN 0885-8950. doi: 10.1109/TPWRS.2006.888988.

Jacek Wasilewski. Integrated modeling of microgrid for steady-state analysis using modified concept of multi-carrier energy hub. *International Journal of Electrical Power and Energy Systems*, 73: 891–898, 2015. ISSN 01420615. doi: 10.1016/j.ijepes.2015.06.022.

Sebastian Long, Alessandra Parisio, and Ognjen Marjanovic. A conversion model for nodes in multi-energy systems. *2017 IEEE Manchester PowerTech, Powertech 2017*, 2017. doi: 10.1109/PTC.2017.7981052.

Getnet Tadesse Ayele, Pierrick Haurant, Björn Laumert, and Bruno Lacarrière. An extended energy hub approach for load flow analysis of highly coupled district energy networks: Illustration with electricity and heating. *Applied Energy*, 212:850–867, dec 2018. ISSN 03062619. doi: 10.1016/j.apenergy.2017.12.090.

Seungwon An, Qing Li, and T.W. Gedra. Natural gas and electricity optimal power flow. *IEEE PES Transmission and Distribution Conference and Exposition*, pages 138–143, 2003. ISSN 1098-6596. doi: 10.1109/TDC.2003.1335171.

Xuezhi Liu, Nick Jenkins, Jianzhong Wu, and Audrius Bagdanavicius. Combined analysis of electricity and heat networks. *Applied Energy*, 162:1238–1250, 2016. ISSN 18766102. doi: 10.1016/j.egypro.2014.11.928.

Albero Martinez-Mares and Claudio R. Fuerte-Esquivel. A Unified Gas and Power Flow Analysis in Natural Gas and Electricity Coupled Networks. *IEEE Transactions on Power Systems*, 27(4): 2156–2166, 2012. ISSN 0885-8950. doi: 10.1109/TPWRS.2012.2191984.

Zhaoguang Pan, Qinglai Guo, and Hongbin Sun. Interactions of district electricity and heating systems considering time-scale characteristics based on quasi-steady multi-energy flow. *Applied Energy*, 167:230–243, 2016. ISSN 03062619. doi: 10.1016/j.apenergy.2015.10.095.

Amin Shabanpour-Haghighi and Ali Reza Seifi. Simultaneous integrated optimal energy flow of electricity, gas, and heat. *Energy Conversion and Management*, 101:579–591, 2015. ISSN 01968904. doi: 10.1016/j.enconman.2015.06.002.

Muditha Abeysekera and Jianzhong Wu. Method for Simultaneous Power Flow Analysis in Coupled Multi-vector Energy Networks. *Energy Procedia*, 75:1165–1171, 2015. ISSN 18766102. doi: 10.1016/j.egypro.2015.07.551.

Xuezhi Liu and Pierluigi Mancarella. Modelling, assessment and Sankey diagrams of integrated electricity-heat-gas networks in multi-vector district energy systems. *Applied Energy*, 167:336–352, 2016. ISSN 03062619. doi: 10.1016/j.apenergy.2015.08.089.

Jordan Jalving, Shrirang Abhyankar, Kibaek Kim, Mark Hereld, and Victor M. Zavala. A graph-based computational framework for simulation and optimisation of coupled infrastructure networks. *IET Generation, Transmission & Distribution*, apr 2017. ISSN 1751-8687. doi: 10.1049/iet-gtd.2016.1582.

Svend Frederiksen and Sven Werner. *No Title*. Studentlitteratur AB, 2014. ISBN 978-91-44-08530-2.

Maunu Kuosa, Kaisa Kontu, Tapio Mäkilä, Markku Lampinen, and Risto Lahdelma. Static study of traditional and ring networks and the use of mass flow control in district heating applications. *Applied Thermal Engineering*, 54(2):450–459, 2013. ISSN 13594311. doi: 10.1016/j.applthermaleng.2013.02.018.

Andrzej J. Osiadacz. *Simulation and analysis of gas networks*. Spon, London, 1987. ISBN 0419124802.

Pieter Schavemaker and Lou Van der Sluis. *Electrical power system essentials*. Wiley, Hoboken, N.J, 2008. ISBN 9780470510278.

Reijer Idema, Domenico Lahaye, Kees Vuik, and Lou Van Der Sluis. Fast Newton load flow. *2010 IEEE PES Transmission and Distribution Conference and Exposition: Smart Solutions for a Changing World*, pages 1–7, 2010. doi: 10.1109/TDC.2010.5484211.

Brian Stott. Review of Load-Flow Calculation Methods. *Proceedings of the IEEE*, 62(7):916–929, 1974. ISSN 15582256. doi: 10.1109/PROC.1974.9544.

B. Sereeter, C. Vuik, and C. Witteveen. On a comparison of Newton-Raphson solvers for power flow problems. Technical Report 17-07, Delft University of Technology, Delft Institute of Applied Mathematics, 2017. URL `http://ta.twi.tudelft.nl/nw/users/vuik/papers/Ser17VW.pdf`.

Chiara Bordin, Angelo Gordini, and Daniele Vigo. An optimization approach for district heating strategic network design. *European Journal of Operational Research*, 252(1):296–307, 2016. ISSN 03772217. doi: 10.1016/j.ejor.2015.12.049.

C. T. C. Arsene, A. Bargiela, and D. Al-Dabass. Modelling and Simulation of Water Systems Based on Loop Equations. *J. of SIMULATION*, 5(1):1–2, 1989. ISSN 1473-8031.

Muditha Abeysekera. *Combined Analysis of Coupled Energy Networks*. PhD thesis, 2016.